Lab on a Chip

PAPER

View Article Online
View Journal | View Issue

Cite this: *Lab Chip*, 2022, **22**, 4327

Rapid prototyping of functional acoustic devices using laser manufacturing†

Xiang Zhang, ‡[a] Rosa Son,‡[a] Yen-Ju Lin,[b] Alexi Gill,[a] Shilin Chen,[cd] Tong Qi,[cd] David Choi,[a] Jing Wen,[d] Yunfeng Lu, [c] Neil Y. C. Lin[aef] and Pei-Yu Chiou*[a]

Received 2nd August 2022,
Accepted 13th October 2022

DOI: 10.1039/d2lc00725h

rsc.li/loc

Acoustic patterning of micro-particles has many important biomedical applications. However, fabrication of such microdevices is costly and labor-intensive. Among conventional fabrication methods, photolithography provides high resolution but is expensive and time consuming, and not ideal for rapid prototyping and testing for academic applications. In this work, we demonstrate a highly efficient method for rapid prototyping of acoustic patterning devices using laser manufacturing. With this method we can fabricate a newly designed functional acoustic device in 4 hours. The acoustic devices fabricated using this method can achieve sub-wavelength, complex and non-periodic patterning of microparticles and biological objects with a spatial resolution of 60 μm across a large active manipulation area of 10 × 10 mm^2.

Introduction

Microparticle and biological cell manipulation and sorting are indispensable in modern biomedical applications. Patterning and sorting based on acoustic fields has been widely studied over the past decade due to its biocompatibility and contactless nature.[1,2] This biocompatibility makes acoustic manipulation the ideal mechanism for many biomedical applications, such as single cell analysis,[3–5] spheroid fabrication,[6–8] drug discovery,[9–11] and tissue engineering.[12–15] Traditional acoustic-based devices utilize bulk acoustic wave (BAW)[16–25] or surface acoustic wave (SAW)[25–36] approaches to pattern acoustic fields. BAW relies on microstructures to form resonant standing waves, which has a limited spatial resolution-typically several hundred micrometers-and limited acoustic modes.[37,38] SAWs are created using interdigitated transducers (IDTs) to form nodes and antinodes and enable the trapping pattern to be changed in real time.[39] However, they have a limited active acoustic manipulation area due to its decaying evanescent wave nature.[40]

Recently, a novel acoustic device called a compliant membrane acoustic platform (CMAP) was shown to exhibit near-field trapping behavior that allowed the patterning of particles at sub-wavelength resolution with complex, non-periodic acoustic potential profiles over a large manipulation area.[37] The basic working principle utilizes a planar acoustic wave generated by a piezoelectric ceramic PZT. This wave passes through a bulk PDMS layer with embedded air cavities and a thin, soft PDMS membrane sitting on top of the bulk PDMS layer (Fig. 1a). The acoustic wave cannot transmit through the air cavities due to the large impedance difference between PDMS and air, while it can transmit through the bulk PDMS structure.[41,42] The difference of the acoustic transmission between the bulk PDMS and air cavity regions creates a near-field acoustic potential gradient for acoustic patterning. A PDMS spacer is placed between the device and another bulk layer of PDMS so that the traveling waves can pass through the water cavity and dissipate in the PDMS material with little reflection. This mechanism has made it possible to trap particles and biological cells at the edges of the air cavities, where the radiation potential is lowest.

While in principle the size of the CMAP device is limited only by the size of the PZT substrate, manufacturing a large-area device proved to be challenging. The previous manufacturing method utilized soft lithography, which relied on a stamping process to fabricate the air cavity structures

[a] *Department of Mechanical and Aerospace Engineering, University of California at Los Angeles, USA. E-mail: pychiou@g.ucla.edu*
[b] *Department of Electrical and Computer Engineering, University of California at Los Angeles, USA*
[c] *Department of Chemical and Biomolecular Engineering, University of California at Los Angeles, USA*
[d] *Department of Microbiology, Immunology and Molecular Genetics, David Geffen School of Medicine, University of California at Los Angeles, USA*
[e] *Department of Bioengineering, University of California at Los Angeles, USA*
[f] *Institute for Quantitative and Computational Biosciences, University of California at Los Angeles, USA*

† Electronic supplementary information (ESI) available. See DOI: https://doi.org/10.1039/d2lc00725h

‡ These authors contribute equally.

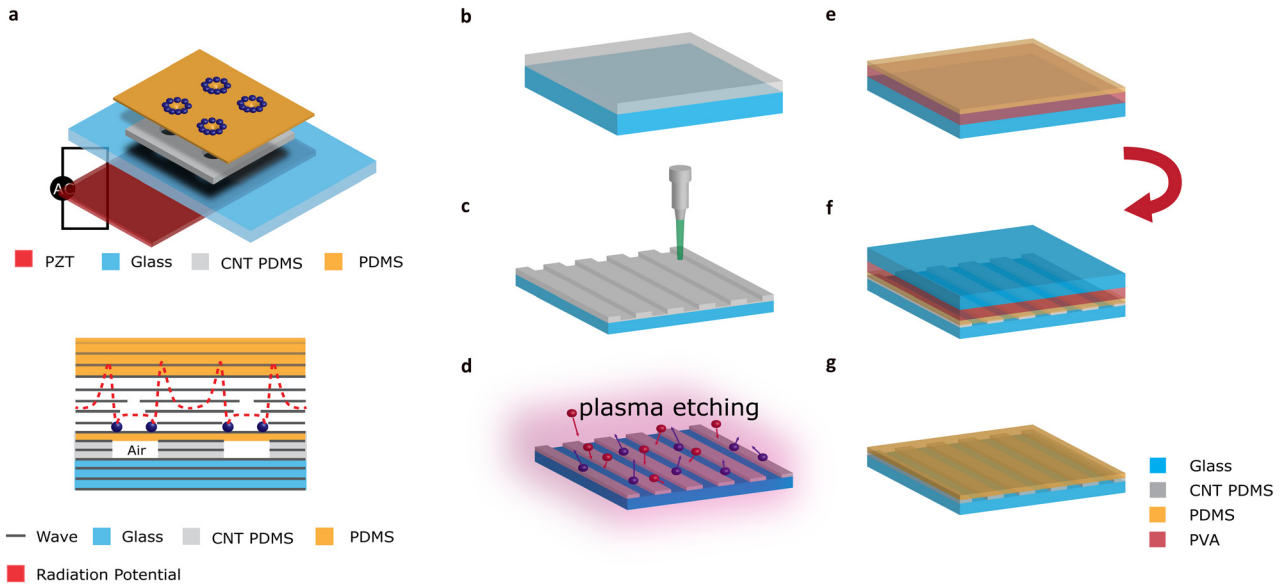

Fig. 1 (a) CMAP device mechanism. A planar acoustic wave is generated from a PZT substrate and propagates upward. The plane wave passes through the PDMS layer while being blocked where it hits the air cavity. This causes a difference in acoustic potential above the air cavity, allowing particles to get trapped in this area. A thick PDMS substrate is placed at the top of the device to allow the acoustic wave to propagate through and decay without reflecting and causing interference with the acoustic pattern. (b–g) Illustration of the process flow for the device. (b) Spin coating of the CNT-PDMS mixture on a glass slide. (c) Laser cutting desired patterns on the CNT-PDMS layer using the 532 nm pulsed laser. (d) Residues on the patterned CNT-PDMS structure are removed by O_2 plasma etching. (e) PVA and PDMS thin membrane layers are spin coated sequentially on another glass slide. (f) Bonding the PDMS thin membrane (on top) with the patterned CNT-PDMS structure (at the bottom) using O_2 plasma treatment on both surfaces. (g) Dissolving the PVA layer in water to release it from glass slide and transfer the PDMS membrane onto the patterned CNT-PDMS structure.

and thin PDMS membrane layer. Transferring the patterned PDMS structure onto a glass substrate was a delicate, challenging, and time-consuming process, as a larger area device with a high aspect ratio compliant membrane made it difficult to transfer with no defects.

In this paper, we present a method for rapid prototyping of CMAP based functional acoustic devices using direct-write laser machining. We have designed a process flow that allows us to rapidly fabricate an acoustic trapping device over a large area and of any arbitrary shape. Laser machining allows for greater versatility and flexibility in pattern generation through computer programming, allowing us to greatly simplify the manufacturing process by eliminating the need for masks or stamps. This rapid prototyping technique allows us to generate a vast number of unique patterns for a fraction of the time and cost of traditional microfabrication techniques.

Results

Device fabrication process

The acoustic device consists of a PZT substrate, glass, a bottom carbon nanotube CNT-PDMS structure, a thin compliant PDMS membrane, and a top PDMS structure. The major fabrication steps for patterning the acoustic device are shown in Fig. 1(b–g). (See the Experimental section for details on the materials and equipment).

To fabricate, the CNT (carbon nanotube) is first measured and submerged in sufficient IPA. Next, the CNT and IPA are ultrasonicated for 1 hour to fully disperse the CNT in the IPA. After, the Sylgard PDMS 527A, Sylgard PDMS 527B and Sylgard PDMS 184A are mixed with the CNT and IPA and then the entire mixture is ultrasonicated again for another 1 hour. Then, the entire mixture is heated on a hot plate at 60 °C for 40 minutes with a magnetic stirrer bar spinning at 500 rpm. When the IPA has nearly evaporated, remove the mixture from the hot plate and add the Sylgard PDMS 184B curing agent into the CNT-PDMS mixture. Once combined, the IPA components from the CNT-PDMS mixture are completely removed and the mixture is degassed until all the trapped air is removed.[43,44] The CNT-PDMS is then spin coated at 3000 rpm onto a 1 mm thick glass slide to result in a 18 μm thick CNT-PDMS film (Measured by Dektak 8 Advanced Development Profiler). The purpose of mixing CNT in the PDMS structure is to increase light absorption for later laser cutting processes.

After curing at 60 °C for 8 hours, the CNT-PDMS mixture is ready to use. The 532 nm wavelength pulsed laser with pulse duration of 25 ns and pulse energy of 130 μJ (measured by a Newport 1835-C & 818-SL optical power meter and power detector) is then used to cut out the desired pattern. While pure PDMS is nearly transparent to the 532 nm wavelength, the CNT-doped PDMS can absorb enough of the laser's energy to be effectively cut through.[45,46] Once the PDMS sample has been patterned, the entire sample is etched using plasma etching (Etch Fluorine-Oxford 80+, SF_6 80 sccm, O_2 20 sccm, 270 W) for 5 minutes to remove residue remaining from the laser ablation.

On a separate glass slide, an aqueous solution containing 14.3% (w/w) water-soluble polyvinyl alcohol (PVA) is spin coated at 2000 rpm to create a thick sacrificial layer and baked at 65 °C for 1 minute and 95 °C for 30 minutes. After baking the PVA, a thin, compliant PDMS layer with a 4 : 1 weight ratio of Sylgard PDMS 527 and Sylgard PDMS 184 is spin coated at 4000 rpm on top of the PVA, which will act as the thin membrane for the acoustic device. This PDMS layer has a thickness of ~4 μm (measured by a Dektak 8 Advanced Development Profiler). Once this is baked at 60 °C for 8 hours, the PDMS membrane is cured and ready to use. After that, both the surface of the PDMS membrane and the CNT-PDMS structure are O_2 plasma treated and bonded. The membrane is then transferred to the CNT-PDMS by dissolving the PVA layer in water to release it from the glass substrate.

Compared with the soft lithography fabrication process in our previous work, this laser manufacturing based rapid prototyping method greatly simplifies the manufacturing process, cost, and time spent per device. Using a direct-write method eliminates the need for a mask or a mold, providing the capability to quickly create and iterate on new designs. This allows us to have a functional acoustic device in hours, rather than days or weeks as was previously the case using our prior fabrication procedures.[35] Such a manufacturing method is especially suitable for academic applications. In addition, this new manufacturing method allows the transfer of a thin membrane onto the acoustic device reliably and repeatedly, without risk of the thin membrane tearing or curling up. In our prior work, the patterned PDMS layer was peeled off and transferred onto the glass substrate by tweezers. However, peeling off the patterned PDMS layer is extremely difficult for two reasons: the thin and soft PDMS layer is very fragile and the thin area curls almost immediately.[47–49] Once the PDMS layer curls, it is near impossible for it to return to its original intended shape, significantly decreasing the throughput of functional devices. These challenges are exacerbated for larger areas. By eliminating the need to peel a thin film from one glass substrate to another, we can create a much larger active device area.

Cutting resolution and limitations

The resolution of the laser patterning technique was evaluated by cutting an array of single beam-width lines of length 500 μm with decreasing space between each cut. The laser passed through the same path for a total of four cuts per line at a cutting speed of 0.5 mm s^{-1}. This cutting speed and number of cuts per line were determined experimentally to be most optimal for cutting through the 18 μm thick CNT-PDMS structure with minimal burning and residue. With these settings, a cutting linewidth of 60 μm and a separation gap smaller than 30 μm has been achieved, as observed in Fig. 2.

Complex, non-periodic acoustic patterning of microparticles

A functional, acoustic trapping device was successfully realized using this rapid laser manufacturing method. The experimental results demonstrate a clear lining of the fluorescent beads at the membrane edges. To test the laser patterning capabilities and demonstrate its versatility, we fabricated a set of structures consisting of representative shapes. All patterns were cut within a 200 × 200 μm^2 area. As shown in Fig. 3a, these patterns include a circle, square, triangle, hourglass, hexagon, and U-shape. These patterns were chosen to demonstrate the potential for cutting future microfluidic channels or acoustic patterning devices. Fig. 3b shows the patterning results of 10 μm fluorescent beads with those patterns.

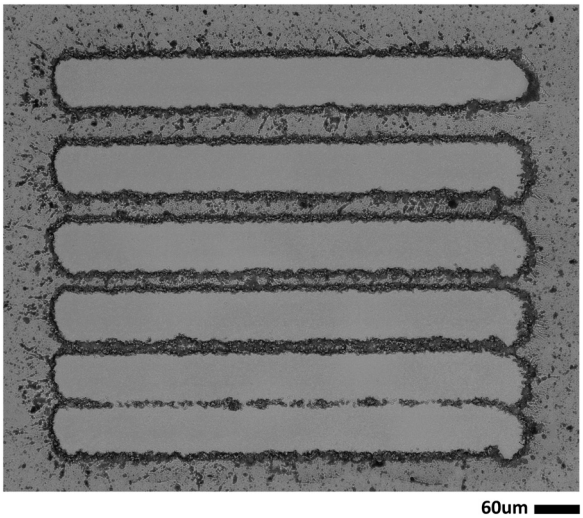

Fig. 2 Single beam width cut at multiple gap spacings. The gap between each cut was digitally programmed between 50 to 90 um, from bottom to top, with each gap increasing by 10 μm. The beam width is about 60 μm. The results shown are after the plasma etching step in Fig. 1d. Scale bar, 60 μm.

Large area device

One of the unique aspects of this manufacturing process is the ability to fabricate large area devices. To test this capability, we have cut an array of 20 1 cm × 250 μm rectangles, spaced 250 μm apart, for a total device area of 10 × 10 mm^2, shown in Fig. 4a. Also, Fig. 4b shows arrays of 150 μm × 150 μm squares, spaced at 300 μm, 150 μm, 100 μm, and 50 μm, for a total device area of 10 × 10 mm^2. As shown in Fig. 4d and e, beads were trapped at the membrane edges across the different sections of the device in Fig. 4a. The trapping results of both squares and rectangles demonstrate the functionality of large area acoustic devices.

Complex, non-periodic patterning of biological samples

Biocompatibility of the laser-manufactured acoustic devices is tested using 2F7-BR44 lymphoma, a type of suspension cell (see the Experimental section part for details on cell culturing). 2F7 cells are stained with calcein AM fluorescent dye for about 30 minutes before doing the experiment. As illustrated in Fig. 5a, patterning of 2F7 cells in the complex

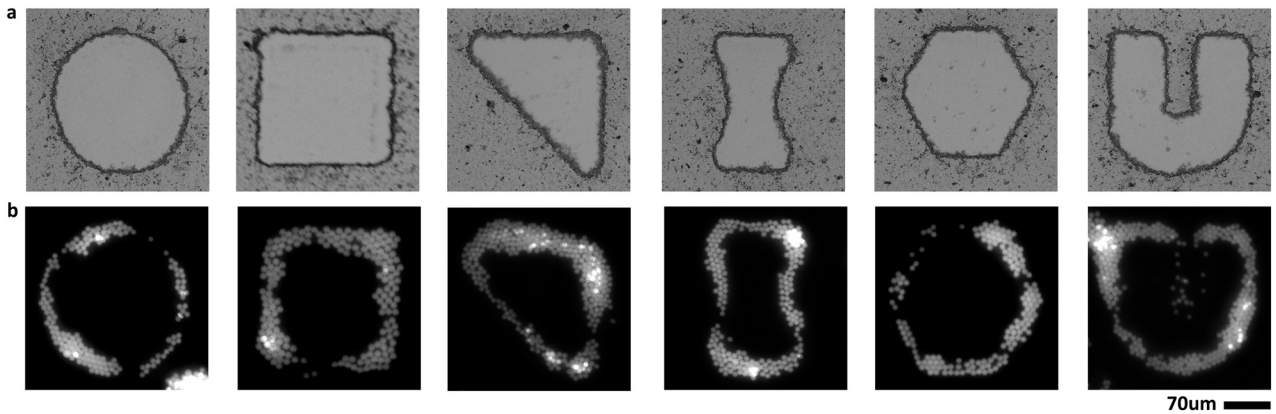

Fig. 3 (a) Arbitrary patterns with a PDMS membrane on top, which were cut within 200 × 200 μm^2 area. (b) Fluorescence images of patterned 10 μm microparticles in water using CNT-PDMS structures for corresponding shapes. Scale bar, 70 μm.

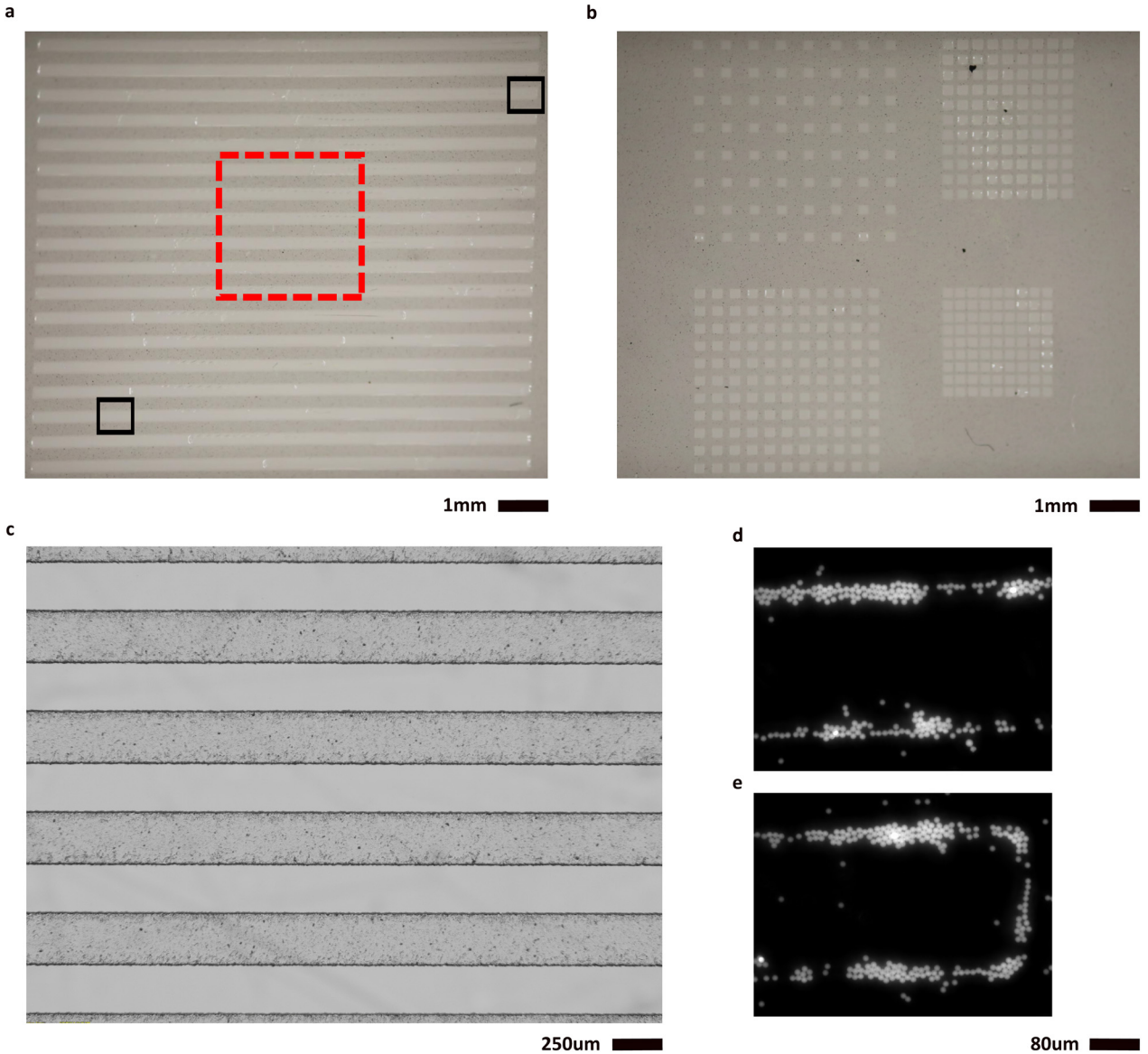

Fig. 4 Large area CNT-PDMS structure device with array of rectangles (a) and array of squares (b). (c) Microscopic images of large area CNT-PDMS structure device marked in the red dashed box in (a). (d) and (e) Fluorescence images of patterned 10 μm microparticles in water marked in the black solid boxes in (a).

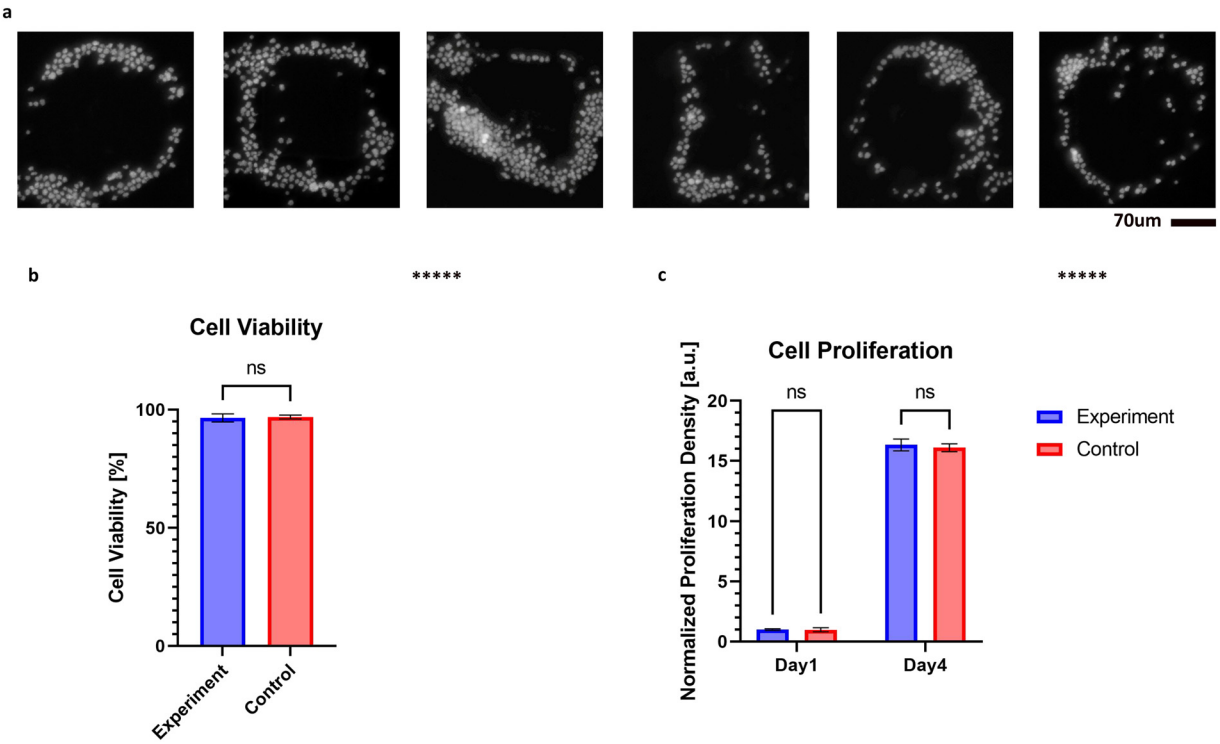

Fig. 5 Patterning and viability assessments of 2F7 cells in IMDM using laser manufactured CNT-PDMS structures for different geometric shapes. (a) Fluorescence images of patterned 2F7 cells stained with calcein AM in IMDM, results are similar with the polystyrene beads in Fig. 3b. (b) Experiment shows comparable cell viability (96.51%) to that of the control (96.86%). (c) Cells from both the control and experiment proliferated by about 16 times after 3 days (72 hours). Scale bar, 70 μm (*****number of trials measured, n = 5, ns: not significant).

and non-periodic shapes resembles that of the polystyrene beads in Fig. 3b.

After 2F7 cells operating in the device at 3 MHz and 5 Vrms for about 5 minutes, a viability assessment using trypan blue (ATCC) and hemocytometer (Hausser Scientific Reichert Bright-Line) is performed. The experimental sample shows a similar level of viability at 96.51% to that of the control group at 96.86%, Fig. 5b. In addition, through unpaired t-test comparison, the p-value between experiment and control group for cell viability is larger than 0.05, which indicates there is no statistical significance between two data sets. Assessment of cell proliferation is also performed to check the biocompatibility. After the experiment, portions of the cells were incubated for 72 hours (from day 1 to day 4). Densities of cells at day 1 and day 4 for both the experiment and control have been approximated by a hemocytometer. All the results indicate an increase about 16 times, shown in Fig. 5c, demonstrating a good biocompatibility of our device. We also conduct unpaired t-test to compare the cell proliferation between experiment and control group and it shows no statistical significance.

Discussion

We have demonstrated rapid prototyping of acoustic devices using laser manufacturing. Our method minimizes the conventional acoustic device fabrication period from a couple days to a couple hours using pre-coated CNT-PDMS film and thin soft PDMS film on PVA substrates that can be prepared in mass and made ready for laser cutting of new designs. Without losing any function, the acoustic devices can achieve sub-wavelength, complex and non-periodic patterning of microparticles and biological objects. The structures can be laser cut into any arbitrary geometry. Additionally, the bonding technique makes transferring large area thin PDMS membranes possible. The spatial resolution is suitable for our current acoustic application. However, we can further improve the spatial resolution by using a high magnification objective lens instead of a single plano-convex lens to shrink the laser beam size. With higher spatial resolution, more complex designs are possible.

In Fig. 3–5, the microparticles and cells distribution on the edge of the air cavities area is not homogeneous. There are a few reasons that can cause this nonuniform distribution near cavity edges. First, acoustic fields between neighboring air cavities can interfere, which perturbs the acoustic field landscape near a cavity. This has been simulated and observed in our prior work.[37] Second, laser-cut PDMS structure does not have a flat and vertical sidewall as the molded PDMS structure using conventional soft lithography. Therefore, bonding between the PDMS membrane and the laser cut structure may not be uniform. This changes the boundary conditions for membrane vibration as well as the particles distribution nearby. The blurry edges also contribute to this effect. We suspect that

the blurry edges are due to the thermal effects caused by nanosecond laser. These edges are greatly impacted by the CNT concentration, with higher concentrations resulting in greater thermal effects. During cutting, the CNT-PDMS mixture melts first and redeposit, making the edges nonuniform. To achieve precise and smooth edges, lasers with even shorter pulse width are needed. Picosecond or femtosecond lasers are suitable for our rapid prototyping in the future. They can heat up the local area rapidly and vaporize materials directly, thus precise and smooth edges can be obtained.

In our application, we were able to sufficiently trap 10 μm beads and biological cells. For manipulating and patterning small particles, acoustic streaming effect needs to be considered since acoustic radiation force scales down with the volume of particle and becomes less dominant on small particles. For example, we have observed that 1 μm particles would circulate near the air cavity edges due to microfluidic vortices induced by acoustic streaming. More studies on the relationship between the radiation force, acoustic streaming, and their relationship with low membrane structure and pillar structure will be needed for future applications.

In addition, tiny black dots are noticeable from the cutting result images in Fig. 3 and 4, resulting from not fully dispersed CNT. Different sizes of CNT chunks influence the image quality. To obtain more homogeneous CNT-PDMS dispersion, dispersing CNT in the IPA by using a probe ultrasonicator instead of an ultrasonic cleaner we currently use could be possible. Without CNT chunks in the CNT-PDMS dispersion, better quality images can be achieved. There is another potential option to solve this issue. As mentioned above, mixing CNT in PDMS is to increase the light absorption for laser cutting. If a UV pulse laser is used, direct PDMS cutting is feasible and would eliminate the need of mixing CNT in PDMS.

Furthermore, our method has great potential in fabricating large-aspect ratio structures, giving us 3D manufacturing capabilities that will allow us to manufacture deep wells of any arbitrary shape and size. By tuning the laser's power, repetition rate, and traveling speed, we can tune the amount of material each pass of the laser will burn through, allowing us to theoretically drill through a specified thickness of a material. In the future, new devices may be designed to utilize this concept for even greater capabilities.

Conclusion

In conclusion, a rapid prototyping method using laser manufacturing has been demonstrated. This rapid prototyping process is capable of fabricating functional acoustic devices in 4 hours. In addition, sub-wavelength, complex and non-periodic patterning of microparticles and biological objects at a spatial resolution of 60 μm across a 10 × 10 mm^2 area can be achieved by the devices fabricated using our method. Higher resolution is possible through reducing the laser beam size. In the future, with the help of UV pulsed laser, PDMS structures could be directly cut instead of mixing CNT, making the fabrication process even easier and the fabricated devices more suitable for optical imaging and observation. Furthermore, by precisely controlling the laser cutting parameters, 3D devices with different PDMS thicknesses at different regions is feasible. The proposed laser manufacturing method has the potential to fabricate unique and versatile microfluidic devices capable of micro-particle patterning, sorting, and advanced 3D manufacturing.

Experimental section

Laser setup

For the device fabrication, the sample was cut using an EKSPLA Jazz 20 DPSS 532 nm laser with a pulse duration of 25 ns, pulse energy of 130 uJ, and repetition rate of 1 kHz. Pulse energy is measured by Newport 1835-C optical power meter and Newport 818-SL optical power detector. A 1 inch plano convex lens was used to focus the beam diameter from 800 um to 60 um. The sample was placed onto a Thorlabs MLS203 high-speed motorized XY scanning stage. A black metal plate was mounted onto a Thorlabs Z825B single axis stage, connected to a Thorlabs TDC001 controller to act as a shutter for the laser. The cutting patterns are programmed using MATLAB v2021b.

Acoustic device operation

The setup for operating the acoustic device is like that in our prior work.[35] It consists of a power amplifier (ENI Model 2100 L), a function generator (Agilent Model 33220A), a T.E. cooler (T.E. Technology Model CP-031HT), an ultra-long working distance microscope lens (20× Mitutoyo Plan Apo), an upright microscope (Zeiss Model Axioskop 2 FS), and a mounted recording camera (Zeiss Model AxioCam mRm). The function generator sends A.C. signals to the signal amplifier, which is electrically connected to the PZT substrate. The PZT will then convert the electrical signals into mechanical waves, which vibrates the substrate and creates acoustic traveling waves that propagate through the device. To prevent potential thermal damage generated by PZT, a T. E. cooler is placed under the device while operating. The device is positioned under the Mitutoyo lens mounted on the Zeiss microscope. A clear bulk PDMS piece is placed on top of the device, allowing for the acoustic patterning mechanism to be clearly observed and recorded using the Zeiss AxioCam.

Materials

The materials needed to fabricate the soft CNT-PDMS structure are (based on Sylgard PDMS 184A weight): 1 wt% CNT (purchased from Cheap Tubes Inc), sufficient Isopropanol (IPA) to submerge the CNT, 100 wt% Sylgard PDMS 527A, 100 wt% Sylgard PDMS 527B, 100 wt% Sylgard PDMS 184A, and 10 wt% Sylgard PDMS 184B (Curing Agent). In our fabrication, we use 2 g for Sylgard PDMS 184A. Other materials are added based on the weight ratio above. To

make polyvinyl alcohol (PVA) solution, prepare 150 g water and heat it up to at least 70 °C (temperature in water) with a stir bar stirring at 500–700 rpm. Gently and slowly pour PVA powder into the beaker. Start to count for an 8-hour stirring process. The temperature is maintained between 88 °C and 90 °C. Filter the solution when it cools down to 50 °C by a 40 μm filter and leave it for 1 to 2 days. All the chemicals were used as received without further purification.

Polystyrene beads

10 μm polystyrene green fluorescent beads are obtained from Thermo Fisher Scientific, USA.

Cell culturing

A 2F7-BR44 lymphoma cell line is obtained from a CNS lymphoma. This cell line was subcloned from the human 2F7 Burkitt NHL cell line, which was retrieved from a patient with AIDS-lymphoma.[50] 2F7 cells are cultured in Iscove's Modified Dulbecco's Medium (IMDM), a modification of Dulbecco's Modified Eagle Medium, supplemented with 10% (vol/vol) fetal bovine serum (FBS, ThermoFisher Scientific) and 1% penicillin/streptomycin (mediatech). 2F7 cells are seeded in T25 Nunclon Sphera Flasks (ThermoFisher Scientific) at a concentration of 5×10^5 cells per mL and are kept in T25 Nunclon Sphera Flasks (ThermoFisher Scientific) in an incubator at 37 °C and 5% CO_2. The medium is changed at 24 hours after seeding and 2F7 cells are isolated and used for experiments after 72 hours of culture.

All experiments were performed in compliance with policies and guidance provided by UCLA Institutional Biosafety Committee (IBC), which is responsible for oversight of all research activities – including teaching laboratories – involving the use of hazardous biological material and recombinant or synthetic nucleic acids, as required and outlined in the NIH guidelines for research involving recombinant or synthetic nucleic acid molecules (NIH Guidelines) and the CDC/NIH Biosafety in Microbiological and Biomedical Laboratories (BMBL). All the experiments were approved by UCLA Institutional Biosafety Committee (IBC) and no experimentation with human subjects was performed.

2F7 Burkitt NHL cell was obtained from the American Type Culture Collection (ATCC; Rockville, MD) (CRL-10237 - Discontinued). After acquisition, 2F7 cells were transduced with a lentiviral vector encoding mStrawberry under ubiquitin C promoter. Transduced 2F7 cells were flow sorted for mStrawberry expression and sub-cloned to obtain single cell clones for the *in vitro* on-chip studies.

Author contributions

X. Z. and R. S. are the main contributors who designed and fabricated device, built the experimental setup, conduct the experiments, analyzed the data, and wrote most of the manuscript. X. Z., R. S., and P.-Y. C. shared the ideas for the project. Y.-J. L. advised on the design of the laser setup and device fabrication process. A. G. assisted conducting the experiments and advised on the materials. S. C., T. Q., and D. C. prepared the 2F7 cells for the experiments, as well as shared their knowledge in cell culturing. W. J., Y. L., and N. L. advised on the cell experiments and provided equipment. P.-Y. C. supervised the project and revised the manuscript.

Conflicts of interest

There are no conflicts to declare.

Acknowledgements

This research is supported by the National Science Foundation NSF CMMI 2029454 and the National Institute of General Medical Sciences (NIGMS) of the National Institutes of Health NIH R01GM127985.

References

1 X. Ding, P. Li, S.-C. S. Lin, Z. S. Stratton, N. Nama, F. Guo, D. Slotcavage, X. Mao, J. Shi, F. Costanzo and T. J. Huang, *Lab Chip*, 2013, **13**, 3626.
2 M. Wu, A. Ozcelik, J. Rufo, Z. Wang, R. Fang and T. Jun Huang, *Microsyst. Nanoeng.*, 2019, **5**, 32.
3 D. Collins, B. Morahan and J. Garcia-Bustos, *et al.*, *Nat. Commun.*, 2015, **6**, 8686.
4 D. Ahmed, A. Ozcelik, N. Bojanala, N. Nama, A. Upadhyay, Y. Chen, W. Hanna-Rose and T. J. Huang, *Nat. Commun.*, 2016, **7**, 11085.
5 F. Guo, Z. Mao, Y. Chen, Z. Xie, J. P. Lata, P. Li, L. Ren, J. Liu, J. Yang, M. Dao, S. Suresh and T. J. Huang, *Proc. Natl. Acad. Sci. U. S. A.*, 2016, **113**, 1522–1527.
6 B. Chen, Y. Wu, Z. Ao, H. Cai, A. Nunez, Y. Liu, J. Foley, K. Nephew, X. Lu and F. Guo, *Lab Chip*, 2019, **19**, 1755–1763.
7 K. Chen, M. Wu, F. Guo, P. Li, C. Y. Chan, Z. Mao, S. Li, L. Ren, R. Zhang and T. J. Huang, *Lab Chip*, 2016, **16**, 2636–2643.
8 Y. Wu, Z. Ao, B. Chen, M. Muhsen, M. Bondesson, X. Lu and F. Guo, *Nanotechnology*, 2018, **29**, 504006.
9 P. Kanigowska, Y. Shen, Y. Zheng, S. Rosser and Y. Cai, *SLAS Technol.*, 2016, **21**, 49–56.
10 E. K. Sackmann, L. Majlof, A. Hahn-Windgassen, B. Eaton, T. Bandzava, J. Daulton, A. Vandenbroucke, M. Mock, R. G. Stearns, S. Hinkson and S. S. Datwani, *SLAS Technol.*, 2016, **21**, 166–177.
11 B. Hadimioglu, R. Stearns and R. Ellson, *SLAS Technol.*, 2016, **21**, 4–18.
12 A. Schiavi, C. Guglielmone, F. Pennella and U. Morbiducci, *Meas. Sci. Technol.*, 2012, **23**, 105702.
13 H. Li, J. R. Friend and L. Y. Yeo, *Biomaterials*, 2007, **28**, 4098–4104.
14 M. L. Fabiilli, C. G. Wilson, F. Padilla, F. M. Martín-Saavedra, J. B. Fowlkes and R. T. Franceschi, *Acta Biomater.*, 2013, **9**, 7399–7409.
15 M. Bok, H. Li, L. Y. Yeo and J. R. Friend, *Biotechnol. Bioeng.*, 2009, **103**, 387–401.

16 J. Greenhall, F. Guevara Vasquez and B. Raeymaekers, *Appl. Phys. Lett.*, 2013, **103**, 074103.
17 B. Raeymaekers, C. Pantea and D. N. Sinha, *J. Appl. Phys.*, 2011, **109**, 014317.
18 E. R. Dauson, K. B. Gregory, I. J. Oppenheim, G. P. Healy and D. W. Greve, *2015 IEEE International Ultrasonics Symposium (IUS)*, 2015.
19 B. Hammarström, T. Laurell and J. Nilsson, *Lab Chip*, 2012, **12**, 4296.
20 I. Leibacher, P. Reichert and J. Dual, *Lab Chip*, 2015, **15**, 2896–2905.
21 C. W. Shields IV, J. L. Wang, K. A. Ohiri, E. D. Essoyan, B. B. Yellen, A. J. Armstrong and G. P. López, *Lab Chip*, 2016, **16**, 3833–3844.
22 J. D. Adams, P. Thévoz, H. Bruus and H. T. Soh, *Appl. Phys. Lett.*, 2009, **95**, 254103.
23 A. Castro and M. Hoyos, *Ultrasonics*, 2016, **66**, 166–171.
24 S. Orbay, A. Ozcelik, J. Lata, M. Kaynak, M. Wu and T. J. Huang, *J. Micromech. Microeng.*, 2016, **27**, 015008.
25 J. Rufo, F. Cai and J. Friend, *et al.*, *Nat. Rev. Methods Primers*, 2022, **2**, 30.
26 A. K. Tay, M. Dhar, I. Pushkarsky and D. Di Carlo, *Lab Chip*, 2015, **15**, 2533–2537.
27 G. Destgeer and H. J. Sung, *Lab Chip*, 2015, **15**, 2722–2738.
28 S.-C. S. Lin, X. Mao and T. J. Huang, *Lab Chip*, 2012, **12**, 2766.
29 L. Y. Yeo and J. R. Friend, *Biomicrofluidics*, 2009, **3**, 012002.
30 A. Akther, S. Marqus, A. R. Rezk and L. Y. Yeo, *Anal. Chem.*, 2020, **92**, 10024–10032.
31 X. Ding, S.-C. S. Lin, B. Kiraly, H. Yue, S. Li, I.-K. Chiang, J. Shi, S. J. Benkovic and T. J. Huang, *Proc. Natl. Acad. Sci. U. S. A.*, 2012, **109**, 11105–11109.
32 X. Ding, S.-C. S. Lin, M. I. Lapsley, S. Li, X. Guo, C. Y. Chan, I.-K. Chiang, L. Wang, J. P. McCoy and T. J. Huang, *Lab Chip*, 2012, **12**, 4228.
33 Y. Bian, F. Guo and S. Yang, *et al.*, *Microfluid. Nanofluid.*, 2017, **21**, 132.
34 Y. Chen, X. Ding, S.-C. Steven Lin, S. Yang, P.-H. Huang, N. Nama, Y. Zhao, A. A. Nawaz, F. Guo, W. Wang, Y. Gu, T. E. Mallouk and T. J. Huang, *ACS Nano*, 2013, **7**, 3306–3314.
35 J. Shi, D. Ahmed, X. Mao, S.-C. S. Lin, A. Lawit and T. J. Huang, *Lab Chip*, 2009, **9**, 2890.
36 J. Nam, H. Lim, D. Kim and S. Shin, *Lab Chip*, 2011, **11**, 3361.
37 K.-W. Tung, P.-S. Chung, C. Wu, T. Man, S. Tiwari, B. Wu, Y.-F. Chou, F.-L. Yang and P.-Y. Chiou, *Lab Chip*, 2019, **19**, 3714–3725.
38 K.-W. Tung and P.-Y. Chiou, *Appl. Phys. Lett.*, 2020, **116**, 151901.
39 A. Ozcelik, J. Rufo, F. Guo, Y. Gu, P. Li, J. Lata and T. J. Huang, *Nat. Methods*, 2018, **15**, 1021–1028.
40 O. Tigli and M. E. Zaghloul, *2010 53rd IEEE International Midwest Symposium on Circuits and Systems*, 2010.
41 J.-H. Lee, K.-J. Lee, H.-G. Park and J.-H. Kim, *Ocean Eng.*, 2015, **103**, 160–170.
42 I. Leibacher, S. Schatzer and J. Dual, *Lab Chip*, 2014, **14**, 463–470.
43 M.-K. Kim, M.-S. Kim, H.-B. Kwon, S.-E. Jo and Y.-J. Kim, *RSC Adv.*, 2017, **7**, 48368–48373.
44 J. H. Kim, J.-Y. Hwang, H. R. Hwang, H. S. Kim, J. H. Lee, J.-W. Seo, U. S. Shin and S.-H. Lee, *Sci. Rep.*, 2018, **8**, 1375.
45 N. E. Stankova, P. A. Atanasov, R. G. Nikov, R. G. Nikov, N. N. Nedyalkov, T. R. Stoyanchov, N. Fukata, K. N. Kolev, E. I. Valova, J. S. Georgieva and S. A. Armyanov, *Appl. Surf. Sci.*, 2016, **374**, 96–103.
46 V. Prajzler, M. Neruda and P. Nekvindová, *J. Mater. Sci.: Mater. Electron.*, 2018, **29**, 5878–5884.
47 D. Bartolo, G. Degré, P. Nghe and V. Studer, *Lab Chip*, 2008, **8**, 274–279.
48 Y. Zheng, W. Dai, D. Ryan and H. Wu, *Biomicrofluidics*, 2010, **4**, 036504.
49 L. Engel, J. Shklovsky, D. Schrieber, S. Krylov and Y. Shacham-Diamand, *J. Micromech. Microeng.*, 2012, **22**, 045003.
50 J. Wen, L. Wang and J. Ren, *et al.*, *J. Immunother. Cancer*, 2021, **9**, e001524.